Non-linearity Simulation of Digital SiPM Response for In-homogeneous Light

S. Kumar, *Member, IEEE*, M. Herzkamp, and S. van Waasen

***Abstract*—Currently we are developing a neutron scintillation detector prototype using silicon photomultipliers (SiPM) as the photodetector. In order to reconstruct the position of single neutron events to a better accuracy than the pixel pitch of the SiPM, a very accurate photon count is required. Each pixel consists of 3200 micro-cells, operated in Geiger mode. A cell which is already triggered cannot detect any following photons hitting the cell, until it is recharged. This leads to a non-linearity in the pixel's response for a higher photon density impinging across the pixel. Previous studies provided a correction factor to estimate the saturation, by assuming a homogeneous photon distribution density and comparing it to the number of micro-cells. In our specific application, the photon distribution is not homogeneous, which is why we examined the influence of the homogeneity on the saturation. In this work, we present a case study for difference in non-linearity effect for an in-homogeneous and homogeneous photon distribution density, given the light intensity is equal. The simulation results suggest that the effect could be higher for an in-homogeneous distribution. Therefore, care must be taken when using the established correction factor for saturation and an analysis of the photon distribution homogeneity is necessary.**

***Index Terms*—Neutrons, Position sensitive particle detectors, Photodetectors, Radiation detectors, Scintillators**

I. Introduction

FOR a long time neutron sensitive glass scintillators have been used to detect thermal and cold neutrons [1]. The distribution of light, produced due to neutron capture in the scintillator, helps to determine the position of the neutron event, following the Anger camera [2] approach. Traditionally, vacuum photomultiplier tubes (PMTs) perform the light detection in such neutron scintillator detectors [3] [4]. In the current development, we use a solid-state photodetector, namely silicon photomultiplier (SiPM), as an alternative to PMTs. The benefits are low cost, low operating voltage, and insensitivity to magnetic field. Despite these advantages, SiPMs are largely ignored in neutron detection applications due to their vulnerability to radiation damage. Nevertheless, findings [5] [6] in the past has suggested an acceptable lifetime and performance of SiPMs for these applications with a dose up to 10^{12} n/cm^2. Therefore, we developed a neutron scintillation detector prototype based on digital SiPM arrays and measured its performance recently [7]. Moreover, a group at LIP, Coimbra [8] has also developed a neutron detector utilizing the SiPM. However, SiPM has already been investigated [9] [10] [11] in positron emission tomography for a potential replacement of PMTs to read out a monolithic scintillator for reconstructing the positions. A similar principle is employed in this work.

In order to achieve the goal of two-dimensional spatial resolution of 1 mm $\times$ 1 mm with the SiPM's pixel pitch of 4 mm, we use a position reconstruction algorithm based on the number of photons measured experimentally by multiple pixels. For the algorithm to work properly, it is important to know the expected number of photons corresponding to a certain neutron position with high accuracy. For a detailed description of the algorithm, we refer the reader to [7].

Due to the micro-cell structure of SiPMs, two or more photons hitting the same cell are counted as a single hit, therefore cause a loss of detected photons that needs to be corrected. This non-linearity in SiPMs is well known and has been studied in detail [12] [13] [14] [15], however all these studies assume a homogeneous distribution of photons across the pixel surface. To the best knowledge of the authors, no study has considered an in-homogeneous distribution. However, in our case the distribution is far from homogeneous. Therefore, we investigate the difference between estimations of non-linearity due to micro-cell saturation, using homogeneous and in-homogeneous photon distributions.

II. Optical Front end

The optical front-end (see Fig. 1) of our neutron detector prototype consists of 1 mm thick GS20® [16], a ^{6}Li-enriched Cerium-doped monolithic scintillator glass, and digital SiPM modules. A light guide is glued between the scintillator and the SiPM array in order to spread the light across multiple pixels of the SiPM array. Additionally, the optical front-end is covered with an aluminum cap, which prevents stray light from entering the detector. A detailed description of the optical front-end can be found in [17], which concluded that a 1.1 mm thick glass of refractive index 1.5 is well suited as the light guide.

The present development uses state-of-the-art digital SiPMs [18], fabricated by *Philips Digital Photon Counting GmbH*, which are equipped with triggering logic and active quenching in each micro-cell, as opposed to a common current output provided by parallel-connected micro-cells in analog SiPMs.

Manuscript submitted on Feburary 06, 2020.

S. Kumar is with Central Institute of Engineering, Electronics and Analytics ZEA-2 – Electronic Systems, Forschungszentrum Jülich GmbH, 52425 Jülich, Germany (telephone: 2461-61-85120, e-mail: s.kumar@fz-juelich.de).

M. Herzkamp is with Central Institute of Engineering, Electronics and Analytics ZEA-2 – Electronic Systems, Forschungszentrum Jülich GmbH, 52425 Jülich, Germany (telephone: 2461-61-8091, e-mail: m.herzkamp@fz-juelich.de).

S. van Waasen is with Central Institute of Engineering, Electronics and Analytics ZEA-2 – Electronic Systems, Forschungszentrum Jülich GmbH, 52425 Jülich, Germany (telephone: 2461-61-9400, e-mail: s.van.waasen@fz-juelich.de) and also with Faculty of Engineering, Communication Systems (NTS), University of Duisburg-Essen, 47057 Duisburg, Germany.

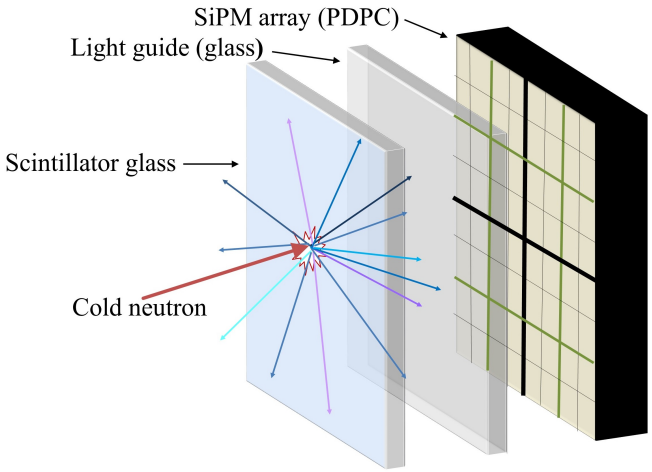

Fig. 1. Expanded view of optical front-end of the detector, representing the isotropic radiation dispersion for the GS20® glass scintillator due to a cold neutron interaction. A light guide is optically coupled to the scintillator to spread the light on to the underlying SiPM array that helps to better locate the position of a neutron, using the reconstruction algorithm.

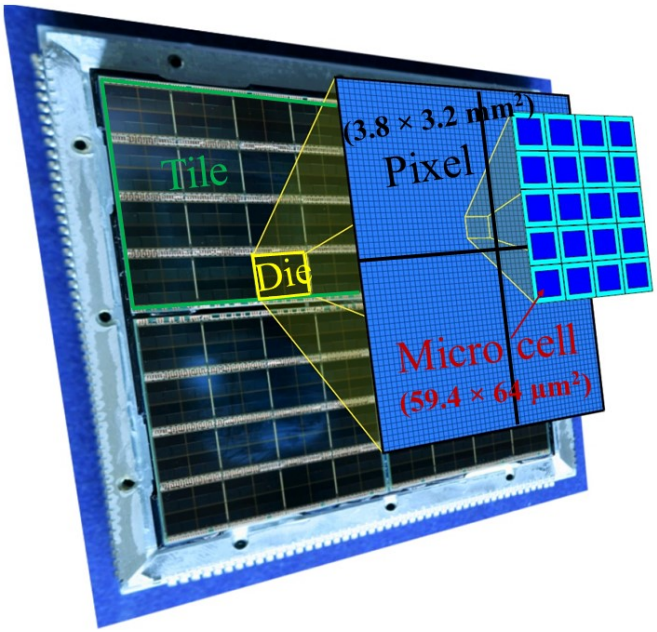

Fig. 2. View of a SiPM module comprised of 2×2 tiles. Each tile has 4×4 dies (independent detection unit) and every die is divided into 2×2 pixels (3.8 mm $\times$ 3.2 mm), each containing 3200 micro-cells (each 59.4 um $\times$ 64 um).

The total active area of the detector is 13.6 cm $\times$ 13.6 cm and consists of a 2×2 array of SiPM modules (65.4 mm $\times$ 65.4 mm).

Each module consists of 2×2 tiles and one tile comprises 64 (8×8) SiPM detection units, referred to as a pixel. Each pixel contains 3200 single photon avalanche diodes (SPADs) referred to as micro-cells here. They are the smallest operating units of a SiPM (see Fig. 2). Every 2×2 array of pixels forms a die, which is an independent readout unit.

The SiPM operates with an event based acquisition system, which is started with an event-triggered signal. Once the trigger scheme is satisfied, the readout cycle initiates the validation of the photon event against the dark count (noise) within the validation interval (35 ns) and after successful validation the sensor enters into photon integration phase (165 ns). During this phase, SiPM waits for more photons from this event. Subsequently, the fired microcells are read out (680 ns) to provide a photon count per pixel and sensor goes to a recharge stage (20 ns) in order to be ready for next event acquisition.

III. Non-Linearity

If a photon triggers a micro-cell, as each micro-cell can only count one photon per acquisition sequence, this micro-cell remains inactive for the remainder of the readout cycle. This means that a second photon hitting the micro-cell cannot be detected, leading to a loss in photon counts. In general, SiPMs respond linearly if the number of photons is significantly lower than the number of micro-cells, otherwise a correction for saturation is required.

After interacting with the scintillator, each neutron creates an event with a decay time of 50 – 70 ns that causes a certain amount of photons to hit the photosensitive surface. Since the whole surface is divided into spatial intervals, i.e. micro-cells, we can assume that the total number of photons n hitting a single micro-cell i during a single neutron event follows a Poisson probability distribution, as correlated noise (crosstalk) is considered negligible.

$$P_i(n) = \exp(-\lambda_i) \cdot \frac{{\lambda_i}^n}{n!} \tag{1}$$

The mean λ_i of this distribution is the expected number of photons hitting the micro-cell during the neutron event. The expected number of fired cells during the event is

$$\langle N_{firedcells} \rangle = N_{cells} - \langle N_{emptycells} \rangle \tag{2}$$

where N_{cells} is the number of cells in a pixel and $N_{emptycells}$ is the number of cells not hit by a photon. If we assume that the statistical processes in different cells are independent of each other, using (1) we have

$$\langle N_{emptycells} \rangle = \sum_i P_i(0) = \sum_i \exp(-\lambda_i) \tag{3}$$

The λ_i are not equal to each other (for in-homogenous photon distribution) and can be calculated by integrating the photon distribution density ρ_{pd} of the neutron event over the micro-cell's area A_i:

$$\lambda_i = P_{PDE} \cdot \int_{A_i} \rho_{pd}\, dr^2 \tag{4}$$

where r is the dimension (x, y) of a micro-cell. Using the common assumption of a homogeneous photon distribution for (2), as decay time is smaller compared to the readout, the Poisson parameters λ_i are all equal to $\frac{P_{PDE} \cdot N_{ph}}{N_{cells}}$, where P_{PDE} is the photon detection efficiency and N_{ph} is the number of impinging photons, we recover the usual non-linearity correction formula:

$$N_{firedcells} = N_{cells}\left(1 - \exp^{\left(\frac{-N_{ph}\cdot P_{PDE}}{N_{cells}}\right)}\right) \quad (5)$$

Once a neutron interacts with the GS20® scintillator, nearly 6000 photons (300 – 500 nm) are created isotropically [16]. Roughly up to 900 photons, taking into account $\approx 31\%$ PDE averaged over the whole spectrum, hit the pixel beneath the neutron event. If distributed homogeneously within the pixel, using (5) we expect around 800 photons to be detected.

For in-homogeneous distribution, which is the case here, the non-linearity correction model for implementation on micro-cell level can be derived using (2) and (3), provided λ_i values are known from (4). For this correction model, we divided the pixel into smaller areas (for e.g. i = 100 microcells), and evaluated the $\langle N_{firedcells}\rangle$ by finding λ_i for the given area.

IV. Simulation

If we had a very thin (e.g. few micrometer) scintillator and neutron pencil-beam scan facility, divergence of the light on the SiPM could have determined experimentally. But this would require lots of resources, especially scanning at such a narrow step (e.g. at microcell level) could be a tedious task. Additionally, the lack of availability of a pencil beam and neutron detection efficiency with a thin scintillator is an issue. Nevertheless, under the present configuration the employed SiPMs do not provide information about which of the micro-cells were triggered, only the total amount, i.e. the pixel counts. Therefore, it was not feasible to measure the photon distribution experimentally. In order to obtain it we instead resort to simulations.

We performed Geant4 [19] simulations of the optical front-end of our prototype detector. Given the geometric layout of the SiPM, we can estimate the number of impinging photons per neutron event and its distribution across the pixel surface.

The simulated model consists of an aluminum slab, the scintillator (13.6 cm × 13.6 cm), a glass light guide and a silicon slab representing the SiPM surface. All components are coupled via thin (0.1 mm) sheets of optical glue. The scintillator parameters, including the decay time (50 – 70 ns), number of photons generated (6000), the scintillation yield etc., were taken from the specifications reported by the manufacturer [16]. We varied the thickness of the light guide in the simulation from 0.0 mm to 2.0 mm in 0.2 mm steps.

For each thickness, we simulated 10,000 cold neutrons (λ = 5 Å, E = 3.27 meV) impinging perpendicularly on the detector surface. The neutrons were absorbed ($\approx 63\%$) within 0.52 mm of GS20® (1 mm thick) [20]. An example of a two dimensional map of photon distribution density is shown in Fig. 3. Obviously, the distribution is in-homogeneous across the area of a single pixel (3.8 mm × 3.2 mm). A peak incident photon density ρ_{pd} of $\approx 130\ photons/mm^2$ around the center of the pixel was observed for 0.2 mm thick light guide (to be compared to the micro-cell density $\approx$ 260 $cells/mm^2$), assuming that a neutron interaction takes place at the center of a pixel.

The simulations were also validated from experimental results for some of the light guide configurations, which show a good agreement for the distribution of the light among the pixels [21].

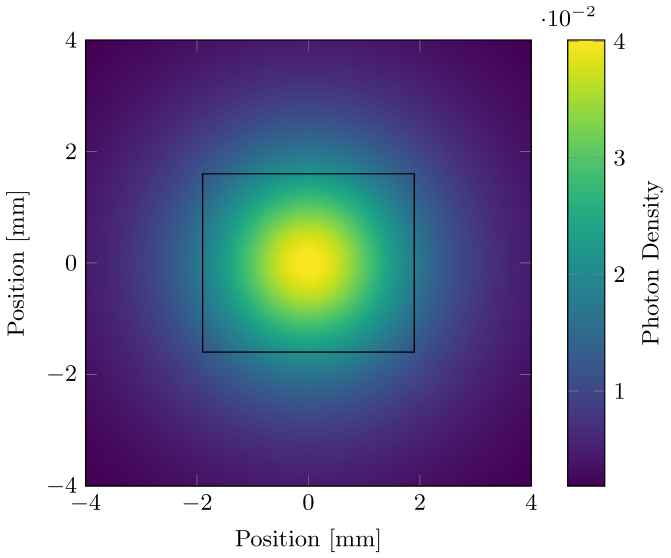

Fig. 3. Photon distribution density, using Geant4 simulation (10,000 neutrons) for 1.1 mm thick light guide for a neutron interaction simulated at (0, 0) mm perpendicularly. The rectangular box in the picture depicts the dimension of a pixel and clearly show the in-homogeneity within it.

In order to determine the N_{ph}, number of photons impinging on micro-cells for in-homogeneous distribution, ρ_{pd} were evaluated from the simulation data and integrated over the area A_i (e.g. a micro-cell) under investigation using (4). Afterwards, the values of λ_i were put in (3) to find $\langle N_{firedcells}\rangle$, that was substituted in (2).

V. Results and Discussion

The figures of merit by which the correction models are compared are the absolute and relative number of photons lost due to micro-cell saturation for different glass thicknesses:

$$N_{lost} = N_{ph}\cdot P_{PDE} - N_{firedcells} \quad (6)$$

$$N_{lost}(\%) = \frac{N_{lost}}{N_{firedcells}}\cdot 100 \quad (7)$$

Fig. 4 shows the figures of merit dependent on the thickness of the light guide. The numbers were calculated assuming a homogeneous (orange and pink) as well as an in-homogeneous (blue and green) photon distribution model. A greater thickness leads to a more homogeneous photon distribution across a single pixel, which is why the difference between both models increases with decreasing thickness of the light guide.

For a 1.1 mm thick light guide (as is the case in our detector design), the difference (0.4%) in the non-linearity models is negligible considering the N_{lost} averaged over a pixel. Therefore, we can use the homogeneous model for non-linearity corrections (5) in our case. However, for zero thickness the difference between both methods (see Fig. 4) was bit higher. Although, this average number is not large on the pixel level, the effect is more pronounced on the absolute scale i.e. microcell level.

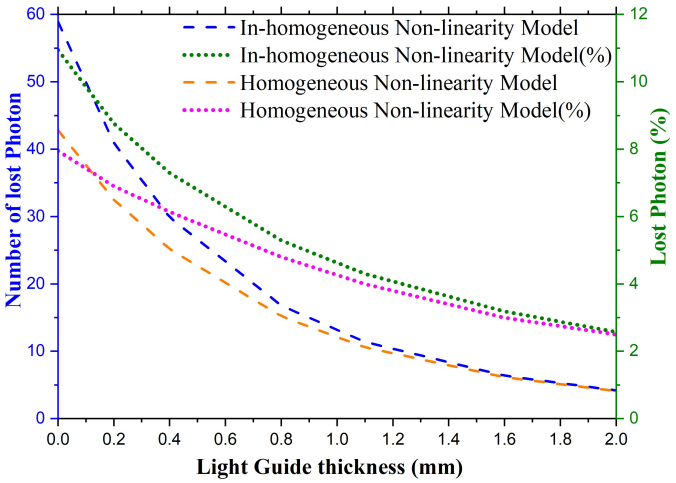

Fig. 4. Graph showing a relation between light guide thickness and the number of photons lost (N_{lost}) averaged over a pixel due to micro-cell saturation, for homogeneous and in-homogeneous photon distribution models.

Fig. 5(a) gives an idea of the spatial distribution of photon loss ratio for a 0.2 mm thick light guide within a pixel, i.e. on micro cell level. The plot spans the area of a pixel with a neutron position in the center. The photon loss reaches almost 24% in the center and falls off toward the pixel edges, whereas for 2.0 mm thick glass, the peak loss observed was only 3% (see Fig. 5(b)). This shows that for a thinner light guide evaluating the non-linearity correction factor using the homogeneous non-linearity model will lead to an error due to the fact of averaging of non-linearity contribution of all the micro-cells in the pixel.

In the case of in-homogeneous light, there could be possibly many sources of error that need to be analyzed before using the in-homogeneous non-linearity model. Generally, factors such as the angle of incidence and position of the neutron relative to the pixel (center or at the edge), and the depth of interaction could result in different outcomes.

A possible approach towards this correction could be developing a detailed 3D model considering the above-mentioned factors and evaluating the expected number of photons using the simulations. Then utilizing this number and the measured photon counts, for the algorithm to reconstruct an image of a known mask [7]. Further, adjusting the model as per the reconstructed image of the mask and achieving the best match after few iterations. However, in realistic situations it will be a time consuming process. Nonetheless, it is advisable to avoid having a configuration of the detector that leads to significant in-homogeneity, due to the difficulties associated with non-linearity corrections.

VI. Conclusion

In our neutron scintillation detector prototype, impinging photon distribution on the photodetector, in our case a digital SiPM array, is not homogeneous. Hence, to investigate the effect of micro-cell saturation that leads to non-linearity we derived the non-linearity correction formula for in-homogeneous light, which utilizes photon distribution density.

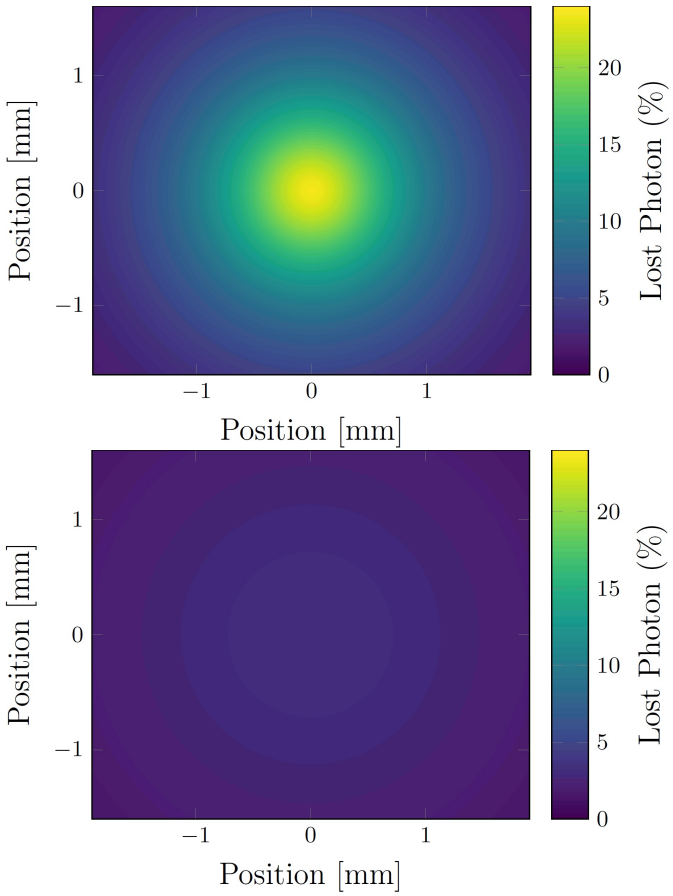

Fig. 5. : Depiction of a two dimensional diagram of photon loss within a pixel (3.8 mm × 3.8 mm) i.e. on micro-cell level, according to the in-homogeneous photon distribution model (a) loss up to 24% for a 0.2 mm thick light guide and (b) up to 3% for a 2 mm thick light guide.

This is analogous to the standard formula used for non-linearity corrections under the assumption of a homogeneous distribution. In order to evaluate the distribution density, one should determine the distribution among the microcell, either via the direct measurement or the simulations that is done here. The former will give more realistic results, provided the aforementioned challenges associated with it are addressed. In addition to that, it will also require a SiPM configuration that can provide data on microcell level.

Based on simulations, we performed a comparison of the models, using the absolute and relative number of photons lost for different light guides used in our optical front-end design. The results clearly show that for a thicker ($>$ 1 mm) light guide the difference between the models is insignificant. But for a thinner light guide the standard non-linearity correction model misrepresents the number of detected photons. In that case, the algorithm being developed, using the probability distribution of all detected photons, to determine the spatial resolution of the detector will provide incorrect results. This leads to a conclusion that the non-linearity correction model derived here under the present circumstances, provides a more accurate estimation of number of detected photons for a SiPM, given the photon distribution within the pixel is highly in-homogeneous.

In general, the authors recommend that for the non-linearity studies in SiPMs not only the number of photons hitting the SiPM, but also their density distribution should be taken into account.

ACKNOWLEDGMENT

The authors would like to thank the member of the ZEA-2 staff: Dr. Carsten Degenhardt and Mr. David Arutinov for the support in this investigation.

REFERENCES

[1] V.K. Voitovetskii, N.S. Tolmavheva, and M.I. Arsaey, *Atomnaya. Energ.* vol. 5, 1959,p. 321; *Atomnaya. Energ.*, vol. 6, 1959, p.472

[2] H. O Anger, "Scintillation camera,"*Review of Scientific Instruments*, Vol. 29, No. 1, 1958, p.27

[3] M. G Strauss, R. Brenner, F. J Lynch, and C. B Morgan , "2-D Position senstive scintillaion detector for neutronsr," *IEEE Transactions on Nuclear Science*, vol. 28, no. 1, 1981, p. 108

[4] R. Riedel, C. Donahue, T. Visscher, and C. Montcalm, "Design and performance of a large area neutron sensitive anger camera," *Nuclear Instruments and Methods in Physics Research A*, vol. 794, 2015, p. 224-233

[5] D. Durini, C. Degenhardt, H. Rongen, A. Feoktystov, M. Schlösser, A- Razo, *et al.*, "Evaluation of the dark signal performance of different SiPM-technologies under irradiation with cold neutrons," *Nuclear Instruments and Methods in Physics Research A*, vol. 835, 2016, p. 99-109

[6] S. Kumar, D. Durini, C. Degenhardt, and S. van Waasen, "Photodetection characterization of SiPM technologies for their application in scintillator based neutron detectors," *Journal of Instrumentation*, vol. 13, no. 1, 2018, Art no. C01042

[7] S. Kumar, M. Herzkamp, C. Degenhardt, J. Seemann, E. Vezhlev and S. van Waasen,"Performance of a Position-Sensitive Neutron Scintillation Detector Based on Silicon Photomultipliers," *IEEE Transactions on Nuclear Science* vol. 67, no. 6, 2020, p. 1169-1174

[8] A. Morozov, J. Marcos, L. Margato, D. Roulier and V. Solovov, "SiPM-based neutron Anger camera with auto-calibration capabilities," *Journal of Instrumentation*, vol. 14, no. 3, 2019, Art. no. P03016

[9] C. Levin, "Design of a high-resolution and high-sensitivity scintillation crystal array for PET with nearly complete light collection," *IEEE Transactions on Nuclear Science*, vol. 49, no.5, 2002, p. 2236-2243

[10] T. K Lewellen, "Recent developments in PET detector technology," *Phys. Med. Biol*, vol. 53, no. 17, 2008, Art. no. R287

[11] D. Schaart, H. Dam, S. Seifert, R. Vinke, P. Dendooven, H. loehner, *et al.* "A novel SiPM-array-based monolithic scintillator detector for PET," *Phys. Med. Biol.*, vol. 54, no.11, 2009, p. 3501-3512

[12] D. Renker, "Geiger-mode avalanche photodiodes, history, properties and problems," *Nuclear Instruments and Methods in Physics Research A*, vol. 567, no.1, 2006, p. 48-56

[13] L. Gruber, S.E. Brunner, J. Marton, and K. Suzuki, " Over saturation behavior of SiPMs at high photon exposure," *Nuclear Instruments and Methods in Physics Research A*, vol. 737, no.1, 2014, p. 11-18

[14] S. Vinogradov, A. Arodzero, R.C. Lanza, and C.P. Welsch, "SiPM response to long and intense light pulses," *Nuclear Instruments and Methods in Physics Research A*, vol. 787, 2015, p. 148-152

[15] Q. Weitzel, P. Bernhard, A.S. Brogna, R. Degele, S. Krause, U. Schäfer, *et al.* "Measurement of the response of Silicon Photomultipliers from single photon detection to saturation," *Nuclear Instruments and Methods in Physics Research A*, vol. 936, 2019, p. 558-560

[16] 6-Lithium glass scintillator for neutron detection (2020, Feb) [Online]. Available: https://scintacor.com/products/6-lithium-glass/

[17] S. Kumar, M. Herzkamp, D. Durini, H. Nöldgen, and S. van Waasen, "Development of a solid-state position sensitive neutron detector prototype based on 6Li-glass scintillator and digital SiPM arrays," *Nuclear Instruments and Methods in Physics Research A*, vol. 954, 2020, Art. no. 161697

[18] T. Frach, G. Prescher, C. Degenhardt, R. de Gruyter, A. Schmitz, and R. Ballizany, "The digital silicon photomultiplier—Principle of operation and intrinsic detector performance," in *IEEE Nucl. Sci. Symp. Conf. Rec. (NSS/MIC)*, Orlando, FL, USA, 2009, p. *1959-1965*

[19] J. Allison,K. Amako, J. Apostolakis, H. Araujo, P. Arce Dubois, M. Asai, *et al.*, "Geant4 Developments and Applications," *IEEE Transactions on Nuclear Science*, vol. 53, no.1, 2006, p. 270-278

[20] C.W.E. van Eijk, A. Bessière, and P. Dorenbos, , "S. Vinogradov, A. Arodzero, R.C. Lanza, and C.P. Welsch, "Inorganic thermal-neutron scintillators," *Nuclear Instruments and Methods in Physics Research A*, vol. 529, 2004, p. 260-267

[21] S. Kumar, M. Herzkamp, and S. van Waasen, "Silicon photomultipliers based neutron detector design: validation of Geant4 simulations," in *SPIE 11114, Hard X-Ray, Gamma-Ray, and Neutron Detector Physics XXI*, San Diego, CA, USA, 2019, p. *111140R*